Beamish Jeffrey (Orcid ID: 0000-0003-4851-3481)
Juliar Benjamin (Orcid ID: 0000-0003-4828-9053)

Deciphering the relative roles of matrix metalloproteinase- and plasmin-mediated matrix degradation during capillary morphogenesis using engineered hydrogels

Jeffrey A. Beamish[1]*, Benjamin A. Juliar[2]*, David S. Cleveland[2], Megan E. Busch[2], Likitha Nimmagadda[2], Andrew J. Putnam[2†]

[1]Division of Nephrology, Department of Internal Medicine, University of Michigan, Ann Arbor, Michigan

[2]Department of Biomedical Engineering, University of Michigan, Ann Arbor, Michigan

* contributed equally to this work

†Corresponding author:

E-mail: putnam@umich.edu (AJP)

This is the author manuscript accepted for publication and has undergone full peer review but has not been through the copyediting, typesetting, pagination and proofreading process, which may lead to differences between this version and the Version of Record. Please cite this article as doi: 10.1002/jbm.b.34341

ABSTRACT

Extracellular matrix (ECM) remodeling is essential for the process of capillary morphogenesis. Here we employed synthetic poly(ethylene glycol) (PEG) hydrogels engineered with proteolytic specificity to either matrix metalloproteinases (MMPs), plasmin, or both to investigate the relative contributions of MMP- and plasmin-mediated ECM remodeling to vessel formation in a 3D-model of capillary self-assembly analogous to vasculogenesis. We first demonstrated a role for both MMP- and plasmin-mediated mechanisms of ECM remodeling in an endothelial-fibroblast co-culture model of vasculogenesis in fibrin hydrogels using inhibitors of MMPs and plasmin. When this co-culture model was employed in engineered PEG hydrogels with selective protease sensitivity, we observed robust capillary morphogenesis only in MMP-sensitive matrices. Fibroblast spreading in plasmin-selective hydrogels confirmed this difference was due to protease preference by endothelial cells, not due to limitations of the matrix itself. In hydrogels engineered with crosslinks that were dually susceptible to MMPs and plasmin, capillary morphogenesis was unchanged. These findings highlight the critical importance of MMP-mediated degradation during vasculogenesis and provide strong evidence to justify the preferential selection of MMP-degradable peptide crosslinkers in synthetic hydrogels used to study vascular morphogenesis and promote vascularization.

KEY WORDS

Capillary morphogenesis, matrix metalloproteinase, plasmin, fibrin, poly(ethylene glycol)

RUNNING HEAD

Matrix remodeling in engineered hydrogels during vasculogenesis

INTRODUCTION

The microvasculature is essential to the normal function, maintenance, and repair of nearly all tissues. This complex network continuously evolves to meet changing demands of tissues. Throughout this process, the extracellular matrix is continuously remodeled, making extracellular proteolytic systems central to the regulation of capillary morphogenesis[1,2].

There are a wide range of proteolytic systems implicated in the formation of new vessels[2]. Matrix metalloproteinases (MMPs), and in particular the membrane-type (MT)-MMPs, have emerged as critical mediators of matrix remodeling not only in collagen but also in fibrin[3-6]. However, the serine protease plasmin, which is also activated at the cell membrane, may provide an alternative mechanism for proteolytic remodeling, and in some conditions, is necessary for capillary morphogenesis in fibrin[7-10]. The relative importance of these systems in capillary morphogenesis therefore remains an open question.

In 3D models, endothelial cells co-cultured with supporting stromal cells undergo capillary morphogenesis[5]. We have observed that stromal cell identity modulates the contribution of the plasmin pathway to this process in fibrin[5,11] and have correlated these observations with differences in the extent of vessel formation, morphology, and permeability both *in vitro*[5,12] and *in vivo*[13]. These findings suggest the mechanisms of proteolytic remodeling during vessel formation may dictate functional properties of the resulting capillary network, which has important implications for the design of synthetic biomaterial scaffolds that support the formation of new vessels.

Deciphering the roles of specific proteolytic pathways has traditionally leveraged molecular genetic tools to create knock-out cells and animals[3,6]. However, redundancies in proteolytic enzyme expression and mechanisms of ECM degradation may complicate interpretations from knock-outs. To complement such approaches, here we used engineered hydrogels[14] with selective degradability to investigate the relative importance of MMP- versus plasmin-dependent ECM degradation during capillary morphogenesis in 3D.

MATERIALS AND METHODS

Cell culture

All reagents were obtained from Thermo Fisher Scientific (Waltham, MA) unless specified. Human umbilical vein endothelial cells (ECs) were harvested from fresh umbilical cords and cultured in fully supplemented EGM2 (Lonza, Walkersville, MD) as previously described[15]. ECs were used between passages 2-4. Normal human dermal fibroblasts (DFs, Lonza) and normal human lung fibroblasts (LFs, Lonza) were cultured in Dulbecco's modified eagle medium (DMEM) supplemented with 10% fetal bovine serum (FBS) and 1% penicillin streptomycin and were used up to passage 15. Bone marrow mesenchymal stem cells (MSCs, RoosterBio, Frederick, MD) were cultured in RoosterNourish-MSC medium (RoosterBio) and used up to passage 5. All cells were cultured at 37 ^{o}C and 5% CO_2 with thrice weekly medium exchange. These cell types were chosen because prior work has suggested they exhibit differential utilization of MMP- and plasmin-mediated proteolysis[5,11].

Fibrin-based vasculogenesis assay with drug inhibitors

A 3D model of capillary morphogenesis was adapted from our previously described protocol [16] as follows. ECs ($1.25x10^5$ cells/mL) and a supportive stromal cell type ($1.25x10^5$ cells/mL) were distributed in 0.5 mL fibrin hydrogels formed in a 24-well culture plate from 2.5 mg/mL of 0.22 μm filtered bovine fibrinogen (Sigma-Aldrich, St Louis, MO) dissolved in serum free DMEM and polymerized with 1 U/mL bovine thrombin (Sigma). After gelation, 1 mL of Vasculife VEGF Endothelial Medium (Lifeline Cell Technology LLC, Frederick, MD) was added to the hydrogel with indicated inhibitors. Aprotinin, derived from bovine lung (Sigma), was added in sterile water at a final concentration 2.2 μM[5], which is nearly 3 orders of magnitude greater than the IC50 for plasmin (4 nM)[17] and has been previously shown to have a saturating effect on capillary morphogenesis[18]. The broad-spectrum MMP inhibitor, GM6001 (Sigma), was supplemented in a constant volume of DMSO vehicle to achieve indicated concentrations.

PEG-VS hydrogel formation

Hydrogels were formed from 4-arm poly(ethylene glycol) vinyl sulfone (PEG-VS; 20 kDa, Jenkem USA, Allen TX) and a combination of thiol containing adhesive and protease-sensitive peptides adapted from published protocols[14,19]. All reagents were prepared in batches of single-use aliquots. Peptides, dissolved in 25 mM acetic acid, and PEG-VS, dissolved in ultrapure water, were 0.22 μm filtered, lyophilized, and stored desiccated at -20 ^{o}C. Precise thiol content of each batch of peptide aliquots was determined using Ellman's reagent. An optimal thiol:vinyl sulfone ratio (typically 0.8-0.9) which yielded the maximum hydrogel shear modulus

was also determined for each batch. Immediately before use, PEG-VS was dissolved in HEPES (100 mM, pH 8.4) and CGRGDS peptide (RGD, Genscript, Piscataway, NJ) was reacted with the PEG-VS for 30 min at a final concentration of 400 μM. In rapid succession, dithiol crosslinking peptides at the optimized thiol:vinyl sulfone ratio (accounting for RGD conjugation) were added to the PEG-VS solution, gently mixed, dispensed into a sterile 0.5 (for 30 μl gels) or 1 mL (50 μl gels) syringe with the needle end cut off, and allowed to polymerize for 1 h at 37 ^{o}C in a sealed 50 mL conical tube. Crosslinking peptides included: Ac-GCRDVPMS↓MRGGDRCG-NH2 ("VPMS"), Ac-GCYK↓NRDCG-NH2 ("YKNR"), Ac-GCYK↓NRDVPMS↓MRGGDRCG-NH2 ("Dual"), and Ac-GCY($_{D}$-K)N($_{D}$-R)DCG-NH2 ("Y$_{D}$-KN$_{D}$-R") each containing an N-terminal acetylation and a C-terminal amidation (Genscript, cleavage site indicated by ↓). Polymerized hydrogels were punched into culture medium or phosphate buffered saline (PBS).

Mechanical and proteolytic characterization of PEG-VS hydrogels

Hydrogels were allowed to swell overnight, then were mounted on an AR-G2 rheometer (TA Instruments, New Castle, DE) between an 8-mm measurement head and a Peltier stage, each covered with P800 sandpaper. Shear storage modulus (G') was determined at 0.05 N normal force, 5% strain amplitude, and 1 Hz frequency and averaged over a 2-minute time sweep. For proteolysis experiments, hydrogels were allowed to swell overnight then transferred to either 5 mU/mL plasmin from human plasma (Sigma) in PBS or to 1 U/mL collagenase IV from *Clostridium histolyticum* (used as a qualitative surrogate for MMP degradation as both MMPs and collagenase IV were found to degrade the VPMS peptide sequence) in PBS supplemented

with 0.4 mM $CaCl_2$ and 0.1 mM $MgCl_2$. Shear modulus was measured at 0, 3, and 24 h. 30 µL hydrogels were used for proteolysis experiments. 50 µL hydrogels were used for all other experiments.

PEG-based vasculogenesis assays

Hydrogels were formed as above except that a cell pellet was resuspended just after adding the dithiol peptide to achieve a final cell density of $2x10^6$ cells/mL of each cell type. 50 µl samples of the resulting suspension were dispensed into 1 mL syringes and polymerized as above. Each hydrogel was cultured in 2 mL of medium in a 12-well plate for 7 d. Either EGM2 or Vasculife VEGF medium were used for these studies. Controls comparing results in both medium types were performed for selected conditions. For the drug inhibitor studies, medium was exchanged daily and inhibitors were added as in the fibrin-based experiments. For all other experiments, medium was exchanged on days 1, 3, and 5.

Fluorescent imaging and quantification methods

On day 7, co-cultures were fixed with Z-fix (Anatech, Battle Creek, MI). All PEG-VS hydrogels were cut down the cylinder diameter prior to staining, yielding two halves. Samples were stained with rhodamine-conjugated lectin from *Ulex europaeus* (UEA, Vector Laboratories, Burlingame, CA, specific for endothelial cells, 1:200), 4', 6-diamidino-2-phenylindol (DAPI, 1 µg/ml, Sigma), and AlexaFluor 488 phalloidin (1:200). PEG-hydrogels were imaged on the cut side to ensure images were representative of cellular behavior within the hydrogels. Images were acquired using an Olympus IX81 microscope equipped with a disk scanning unit (DSU,

Olympus America, Center Valley, PA) and Metamorph Premier software (Molecular Devices, Sunnyvale, CA). For all analyses, confocal z-stacks were acquired using the DSU. Z-series were collapsed into maximum intensity projections prior to analysis. Quantifications of vessel and nuclei densities were performed on 300 μm stacks (30 μm/slice) imaged at 4x. Total vessel length per region of interest (ROI) was quantified using the Angiogenesis Tube Formation module in Metamorph and reported as vessel length per volume of ROI (2.16 x 1.65 x 0.3 mm). Total nuclei per ROI was quantified using a custom ImageJ script (included in supplement). Cell body circularity and projected cell area per volume of ROI were quantified from 30 μm thick stacks (3 μm/slice) imaged at 10x with a custom ImageJ script (included in supplement). For each sample, 6 ROIs were used to determine a mean for each of 3 independent experiments.

Statistics

Statistical analysis was performed using GraphPAD Prism (La Jolla, CA). Unless noted, data are represented as mean ± standard deviation of at least 3 independent experiments. Data were analyzed using one- or two-way ANOVA with Tukey post-hoc testing for pre-specified comparisons. A value of $\alpha < 0.05$ was considered significant.

RESULTS

Synergistic restriction of vasculogenesis by broad spectrum inhibition of MMP- and serine protease-dependent pathways is stromal cell dependent.

We first investigated how inhibition of MMP-dependent and plasmin-dependent fibrinolysis affected capillary morphogenesis in a model of vasculogenesis in which ECs were

distributed with DFs, LFs, or MSCs for 7 d in fibrin hydrogels. The extent of baseline capillary morphogenesis depended on stromal cell identity, with the length of networks in EC-MSC co-cultures 50% and 39% compared to EC-LF or EC-DF co-cultures respectively (Fig 1 and Fig S1). Baseline capillary morphogenesis was unaffected by vasculogenic medium used (Fig S2). GM6001, a broad-spectrum inhibitor of MMPs, consistently reduced vessel formation in a dose-dependent manner regardless of stromal cell identity (Fig 1 and Fig S1, $p < 0.0001$ by two-way ANOVA). Aprotinin, a broad-spectrum inhibitor of serine-proteases including plasmin, similarly tended to reduce vessel formation regardless of stromal cell identity (Fig 1, $p < 0.05$ by two-way ANOVA). The magnitude of the effect, however, was comparatively subtle for EC-MSC co-cultures (Fig 1D). In the absence of GM6001, aprotinin did not affect vessel density. However, the combination of aprotinin and GM6001 revealed a synergistic inhibitory effect from aprotinin that depended on GM6001 concentration for EC-DF and EC-LF co-cultures (two-way ANOVA interaction term $p = 0.035$ and 0.0009, respectively) but not MSCs ($p = 0.46$, Fig 1 and Fig S1). In EC-LF and EC-DF co-cultures, concentrations of GM6001 that were orders of magnitude greater than the nM IC50 range for most MMPs[20] were insufficient to fully inhibit capillary morphogenesis unless aprotinin also was present. Because inhibition of either protease system alone was insufficient to block capillary morphogenesis, these results support a model of partial proteolytic plasticity for vasculogenesis in EC-fibroblast co-cultures in fibrin.

We also evaluated whether aprotinin and GM6001 induced changes in cell spreading and proliferation. The effects of protease inhibition on combined cell density (both EC and stromal

cell) closely mirrored vessel density (Fig S3). Qualitatively, protease inhibition affected spreading of endothelial cells more than stromal cells. Aprotinin and maximal GM6001 severely attenuated, but did not completely block, spreading of any stromal cell type (Fig S4).

Direct matrix degradation by plasmin is insufficient to support robust capillary morphogenesis.

To investigate the hypothesis that fibroblasts induce both MMP- and plasmin-mediated matrix remodeling during capillary morphogenesis, we generated synthetic extracellular matrices using 4-arm PEG-VS crosslinked with peptides selectively degradable nearly exclusively by either MMPs or plasmin (Fig 2A)[14,19]. Hydrogels formed from PEG-VS crosslinked with YKNR were rapidly degraded by plasmin as assessed by loss of shear modulus over time, while equivalent hydrogels formed from either a negative control peptide synthesized with the D-isomer of lysine and arginine (Y_{D}-KN_{D}-R) or VPMS were unaffected by plasmin after 24h (Fig 2B). Inclusion of aprotinin at 2.2 μM prevented YKNR-hydrogel degradation by plasmin, resulting in gels with G' values of 141 ± 10 Pa after 24 hours ($p=0.42$ compared to untreated YKNR control). Taken together, these data show that plasmin exclusively degrades YKNR hydrogels.

Because DFs are readily available from skin and therefore may represent a viable cell source for engineered microvascular constructs, we selected this stromal cell type for further investigation in engineered PEG-VS hydrogel matrices. When ECs and DFs were co-encapsulated within plasmin-sensitive YKNR hydrogels with formulations similar to our prior

work (~40 mg/mL PEG-VS)[14], there was no clear evidence of capillary morphogenesis. By contrast, capillary-like structures were observed in MMP-sensitive VPMS hydrogels (Fig 3A and 3B). To investigate the possibility that vasculogenesis was limited by a grossly supraphysiologic number of matrix cleavage sites, we reduced the concentration of PEG-VS to generate hydrogels with decreasing crosslink density, as assessed by shear rheology[21], to the practical limits of gelation (G' range for 27 mg/mL PEG-VS hydrogels 37 to 61 Pa, Fig 3C). This approach reduced the number of proteolysis events required for local hydrogel dissolution as well as diffusion restrictions. Hydrogel crosslinking, assessed by shear rheology, did not depend on the crosslinking peptide identity (p= 0.30, Fig 3C). In loosely crosslinked YKNR hydrogels, we observed rare areas of minimal capillary morphogenesis (Fig 3A and 3B), but the formation of capillary-like structures was never as robust as observed in VPMS crosslinked hydrogels. Quantified vessel density in 27 mg/mL YKNR hydrogels was similar to that seen in Y_{D}-KN_{D}-R controls (Fig 3B, p= 0.42). In VPMS hydrogels, vessel density was greater in 27 mg/mL compared with 40 mg/mL (Fig 3B, p = 0.008). Capillary morphogenesis in VPMS hydrogels did not depend on the vasculogenic medium used (Fig S5).

To confirm that cell-mediated degradation is possible in plasmin-selective hydrogels, we examined cell spreading in EC-dermal fibroblast co-cultures (Fig 4A) and quantified cell circularity as a measure of cell spreading (Fig 4B). Circularity discriminates rounded versus spread cells (values of 1 indicate perfectly round cells, lower circularity indicates increased elongation). Circularity was low for a large fraction of cells in all VPMS and loosely-crosslinked

YKNR hydrogels but was near 1 for most cells in 40 mg/mL YKNR hydrogels (Fig 4B). The lack of spreading in any Y_D.KN_D.R hydrogels indicated cell spreading depended on matrix degradation (Fig 4B). Qualitatively, we noted cell spreading in YKNR hydrogels predominantly occurred in UEA negative fibroblasts (Fig 4A), suggesting EC spreading was disproportionately restricted in plasmin-selective hydrogels.

Hydrogels with dual susceptibility to both plasmin and MMPs do not enhance vasculogenesis compared with MMP-selective hydrogels.

Our results to this point suggested that plasmin-mediated matrix remodeling was not sufficient to support capillary morphogenesis but did not rule out the possibility that plasmin may have an auxiliary role, perhaps partially degrading the matrix ahead of vessel invasion to facilitate localized MMP mediated degradation. To assess this possibility, we generated a synthetic ECM in which each crosslink could be degraded either by MMPs or by plasmin using a concatenated YKNR+VPMS dual susceptible peptide (Fig 5A). Hydrogels crosslinked with the dual susceptible peptide were degradable by both plasmin and collagenase (used as a surrogate for MMP-mediated degradation) (Fig 5B) and had shear moduli similar to VPMS controls (Fig 5C). EC-DF cocultures in dual susceptible hydrogels resulted in vessel density, projected cell area, and nuclei density equivalent to gels crosslinked with the VPMS peptide (Fig 5D, 5E, 5F).

Synergistic restriction of vasculogenesis by broad spectrum inhibition of MMP- and serine protease-dependent pathways is abolished in MMP-sensitive hydrogels.

Since plasmin can activate soluble MMPs, including those involved in capillary morphogenesis[1], another potential explanation for the reduced vasculogenesis in fibrin cultures containing aprotinin may be inhibition of plasmin-dependent activation of MMPs. To investigate this possibility, inhibition experiments similar to those shown in Fig 1 were repeated in VPMS crosslinked PEG-VS hydrogels that could only be degraded by MMPs. Similar to results in fibrin, GM6001 reduced vessel formation in a dose dependent manner (Fig 6, two-way ANOVA $p = 0.0003$). However, unlike in fibrin, we observed no meaningful differences in vasculogenesis when aprotinin was added to cultures containing GM6001 (Fig 6, two-way ANOVA, aprotinin effect $p = 0.21$, interaction $p = 0.75$).

DISCUSSION

The goal of these studies was to implement a biomaterial engineering approach to investigate the relative importance of plasmin- and MMP-mediated matrix degradation in capillary morphogenesis. Our previous work has suggested that the identity of stromal cells used to support capillary morphogenesis influences the relative importance of MMP- and plasmin-dependent matrix remodeling in fibrin[5,11]. These differences correlate with vessel function[5,12,13]. Therefore, determining the relative roles of plasmin and MMPs in capillary morphogenesis may have critical implications for neovessel function and in the design of biomaterial scaffolds to support vascularization.

First, we investigated whether stromal-cell-dependent differences in the mechanism of proteolysis in fibrin hydrogels observed in angiogenesis models[5,11] extended to a model of

vasculogenesis. This model mimics vascularization strategies often deployed for tissue engineering applications that involve injection of populations of cells[13,14] or pre-patterned cell aggregates[22,23] that organize into microvasculature. The phenotype and angiogenic potential of microvascular ECs[24,25] and stromal cells[5,11-13,26] vary widely according to their origin. We chose umbilical vein-derived ECs and supporting cells derived from bone marrow, lung, and dermis to explore in our model because our prior work has suggested differential utilization of MMP- and plasmin-mediated proteolysis with these combinations[5,11]. Furthermore, this EC source has been utilized widely for understanding mechanisms of capillary morphogenesis[27]. Though we did not specifically test ECs from other origins, an essential role for MMPs in capillary morphogenesis has been described for microvascular[3,28], macrovascular[3,5], and stem cell-derived[25] ECs as has a role for plasmin with ECs derived from both macrovascular[5] and microvascular sources[7-10]. As a result, we anticipate that programs of proteolytic remodeling implied by our investigation are likely generalizable to endothelium from a variety of origins.

For EC-fibroblast co-cultures in this model, we observed 1) a synergistic inhibition of capillary morphogenesis between aprotinin and high concentrations of GM6001 ($\geq$ 10 μM) and 2) robust inhibition required both inhibitors. In contrast, GM6001 alone was sufficient to block capillary morphogenesis in EC-MSC co-cultures. These results suggest that fibroblasts can induce a program of capillary morphogenesis that utilizes both MMP- and plasmin-dependent mechanisms of matrix remodeling consistent with our prior observations[5,11]. The observed IC50 for GM6001 for capillary morphogenesis, regardless of stromal cell identity, was approximately

1 μM. This level is at least two orders of magnitude greater than the IC50 for most MMPs[20], suggesting that inhibition of capillary morphogenesis, and thus any evidence of escape from MMP inhibition due to pericellular plasmin activity, does not occur until MMP activity is fully abolished. While it is possible the observed aprotinin-GM6001 synergy represents off-target effects from the single inhibitor used for each enzyme class in these studies, the fact that similar findings have been observed with a wide range of inhibitors for both MMPs and plasmin pathways in similar models[4,5,11,25] suggests this explanation is unlikely. Together, these results suggest that plasmin can act as a pericellular protease only in circumstances in which the preferred MMP-dependent pathway is essentially inactivated, highlighting the essential role MMPs play.

To investigate the role of plasmin further, we designed synthetic PEG hydrogel ECMs[14,19] in which matrix degradation was selectively limited to MMP- or plasmin-mediated mechanisms by crosslinking the scaffold with protease-selective peptides. We selected the peptide sequences VPMSMRGG (denoted VPMS), which can be degraded by a variety of MMPs (MT1-MMP and MMPs 1, 2, 3, 7, and 9)[29], support cell invasion[30], and support capillary morphogenesis[14] and YKNR, which is plasmin-sensitive and previously optimized for Michael addition reactions[31]. Although this approach provides a selectively degradable ECM model, PEG-VS hydrogels lack many of the pro-angiogenic properties of fibrin, which include a fibrous architecture, macroporous features, binding sites for multiple cell adhesion molecules other than RGD, and binding sites for a variety of growth factors[32]. Also, cells encapsulated in PEG-VS

were never exposed to thrombin, which can activate endothelial cells, though the short duration of exposure in our study (30 min) leads to minimal EC activation[33] and is unlikely to have a meaningful impact over a 7 d culture period. Furthermore, soluble proteases may play an important role in cell-mediated degradation and migration in peptide crosslinked PEG-based hydrogels[34,35]. This property may restrict capillary morphogenesis, which requires membrane bound MT1-MMP in natural ECMs[3]. Despite these limitations, capillary morphogenesis occurred in all VPMS-crosslinked hydrogels. However, a higher initial cell density was needed (targeted at the typical final cell density observed in fibrin gels) and the resulting capillary-like networks were never as extensive as in fibrin.

Initially, in formulations similar to our previous work (40 mg/mL[14]), we observed that spreading of both ECs and stromal cells was severely restricted in YKNR-crosslinked hydrogels. This observation is potentially explained by the fact that PEG-VS hydrogels have a nanoscale architecture with a mesh size on the order of 10-100 nm, in contrast to micron-scale pores in fibrin[36]. As a result, the number of pericellular crosslinks that require degradation to permit cell spreading is at least 400 times greater in 40 mg/mL PEG-VS hydrogels compared with 2.5 mg/mL fibrin (estimated using the starting concentrations of each material, with 2 degradation events per PEG-VS molecule and 1 degradation event per fibrin molecule[37] needed for network dissolution). We also previously observed significant diffusion restrictions in these hydrogels for larger molecular weight molecules similar in size to plasminogen[14], which is supplied by serum

in our vasculogenic culture medium and is a necessary precursor to plasmin-mediated proteolysis.

To overcome these limitations, we generated PEG-VS matrices near the limits of gelation to reduce the number of pericellular crosslinks and minimize diffusion restrictions. In these loosely crosslinked YKNR hydrogels, we observed invasion of the surrounding matrix by fibroblasts. A persistent lack of spreading in control plasmin-insensitive Y_D-KN_D-R hydrogels confirmed cell spreading depended on degradation of the YKNR peptide. These observations indicated that limitations in vasculogenesis could be attributed to differences in the proteolytic preferences of endothelial cells rather than gross limitations in matrix degradability or plasminogen diffusion. This observation that plasmin-mediated degradation requires the PEG-VS hydrogel scaffold to be near the gelation point also may explain conflicting reports regarding the ability of fibroblasts to degrade YKNR crosslinked PEG hydrogels[31,36]. However, only in very loosely crosslinked YKNR hydrogels did we begin to observe occasional rudimentary vasculogenesis, which was never seen in similar soft control Y_D-KN_D-R hydrogels. In contrast, very soft control hydrogels crosslinked with VPMS tended to support more robust network formation, suggesting a correlation between MMP-degradability and vasculogenesis that highlights the dominant role of MMPs in capillary morphogenesis.

These findings are also consistent with other studies noting that increasing crosslink degradability[38] or a more loosely crosslinked network structure[39] correlate with increased capillary morphogenesis. Furthermore, in adipocyte-derived stem cell-EC cocultures, others have

observed evidence that plasmin-mediated ECM degradation becomes increasingly important in densely crosslinked fibrin[18]. Consequently, we hypothesized that plasmin may partially degrade the fibrin network rendering it more susceptible to MMPs and thus facilitating vasculogenesis. To evaluate this hypothesis, we generated PEG hydrogels where each crosslink was susceptible to either MMPs or plasmin by merging both the VPMS and YKNR peptides sequences. These hydrogels were indistinguishable from VPMS-crosslinked controls, both in initial physical properties and in their ability to support capillary morphogenesis. These findings suggested that partial ECM-degradation by plasmin did not contribute significantly to capillary morphogenesis and that the kinetics of ECM remodeling were dominated by MMPs in our PEG-hydrogel co-culture system.

A possible explanation of the apparent role of plasmin-dependent pathways in fibrin hydrogels (based on inhibitor studies) but the failure of capillary morphogenesis in selectively plasmin-sensitive ECMs is that plasmin's role does not involve direct matrix degradation. Plasmin is a potent activator of MMP-3, which in turn activates MMP-9 to increase cellular invasiveness[40]. If indirect plasmin-mediated activation of MMPs contributed to vasculogenesis, then we hypothesized that we should observe a synergy between aprotinin and GM6001 not only in fibrin but also in VPMS hydrogels. Moreover, the VPMS peptide is 8-times more sensitive to cleavage by MMP-9 than MT1-MMP[29], which is of critical importance in vessel formation[4,5], making VPMS hydrogels an ideal environment to test this hypothesis. However, our experiments

demonstrated no synergy between GM6001 and aprotinin in VPMS PEG-VS hydrogels, again highlighting the importance of MMPs alone.

There are several other possible explanations for the observed GM6001-aprotinin inhibition synergy in fibrin which we did not investigate further. Plasmin binding to $\alpha_v\beta_3$ on endothelial cells has been shown to induce endothelial migration[41], offering a potential alternative mechanism by which it may stimulate angiogenesis. Aprotinin also inhibits other serine proteases. Kallikrein, which is synthesized and secreted by ECs and cleaves kininogens into pro-angiogenic kinins[42], may also be present and inhibited at the concentration of aprotinin utilized here (IC50 1-100 nM[43]) to reduce capillary morphogenesis under conditions of MMP inhibition.

Taken together, these results emphasize the utility of engineered ECM mimetics to better understand the mechanisms by which the ECM regulates complex morphogenetic programs in 3D. In particular, our results underscore the essential role for MMP-mediated ECM degradation during capillary morphogenesis and generalize the findings of prior studies in fibrin and collagen hydrogels[3-6] to a precisely defined synthetic ECM. In contrast, our findings do not support a role for plasmin-mediated matrix remodeling in capillary morphogenesis, but instead suggest plasmin may contribute only under very limited circumstances (e.g. in fibrin with near complete MMP inhibition or in situations of supraphysiologic fibrin concentration[18]); such circumstances are unlikely to be physiologically significant. Our model also provides a tool to investigate matrix remodeling in organotypic capillary morphogenesis with specific EC and stromal cell

combinations. Finally, the unique matrix-centric perspective of these studies provides strong evidence to justify the preferential selection of MMP-degradable peptide crosslinkers in synthetic hydrogels used to study vascular morphogenesis[38,39,44-49] and promote vascularization.

Acknowledgments

Research reported in this publication was supported by the National Heart, Lung, and Blood Institute of the National Institutes of Health under Award Number R01-HL085339. JAB was partially supported by the Kidney Research Training Program (T32-DK007378). BAJ was partially supported by the Tissue Engineering and Regeneration Training Program at the University of Michigan (T32-DE007057). The content is solely the responsibility of the authors and does not necessarily represent the official views of the National Institutes of Health.

REFERENCES

1. Ghajar CM, George SC, Putnam AJ. Matrix metalloproteinase control of capillary morphogenesis. Critical reviews in eukaryotic gene expression 2008;18(3):251-278.
2. Hinsbergh VWv, Engelse MA, Quax PH. Pericellular proteases in angiogenesis and vasculogenesis. Arteriosclerosis, thrombosis, and vascular biology 2006;26(4):716-28.
3. Chun T-H, Sabeh F, Ota I, Murphy H, McDonagh KT, Holmbeck K, Birkedal-Hansen H, Allen ED, Weiss SJ. MT1-MMP–dependent neovessel formation within the confines of the three-dimensional extracellular matrix. The Journal of Cell Biology 2004;167(4):757-767.
4. Hiraoka N, Allen E, Apel IJ, Gyetko MR, Weiss SJ. Matrix Metalloproteinases Regulate Neovascularization by Acting as Pericellular Fibrinolysins. Cell 1998;95(3):365-377.
5. Ghajar CM, Kachgal S, Kniazeva E, Mori H, Costes SV, George SC, Putnam AJ. Mesenchymal cells stimulate capillary morphogenesis via distinct proteolytic mechanisms. Experimental cell research 2010;316(5):813-825.
6. Kachgal S, Carrion B, Janson IA, Putnam AJ. Bone marrow stromal cells stimulate an angiogenic program that requires endothelial MT1 -MMP. Journal of Cellula Physiology 2012;227(11):3546-3555.
7. Pepper MS, Belin D, Montesano R, Orci L, Vassalli JD. Transforming growth factor-beta 1 modulates basic fibroblast growth factor-induced proteolytic and angiogenic properties of endothelial cells in vitro. The Journal of Cell Biology 1990;111(2):743-755.

8. Koolwijk P, Erck MGv, Vree WJd, Vermeer MA, Weich HA, Hanemaaijer R, Hinsbergh VWv. Cooperative effect of TNFalpha, bFGF, and VEGF on the formation of tubular structures of human microvascular endothelial cells in a fibrin matrix. Role of urokinase activity. The Journal of Cell Biology 1996;132(6):1177-1188.

9. Oh CW, Hoover -Plow J, Plow EF. Journal of Thrombosis and Haemostasis 2003;1(8):1683-1687.

10. Vogten JM, Reijerkerk A, Meijers JCM, Voest EE, Rinkes IHMB, Gebbink MFBG. The Role of the Fibrinolytic System in Corneal Angiogenesis. Angiogenesis 2003;6(4):311-316.

11. Kachgal S, Putnam AJ. Mesenchymal stem cells from adipose and bone marrow promote angiogenesis via distinct cytokine and protease expression mechanisms. Angiogenesis 2011;14(1):47-59.

12. Grainger SJ, Putnam AJ. Assessing the Permeability of Engineered Capillary Networks in a 3D Culture. PLoS ONE 2011;6(7).

13. Grainger SJ, Carrion B, Ceccarelli J, Putnam AJ. Stromal Cell Identity Influences the In Vivo Functionality of Engineered Capillary Networks Formed by Co-delivery of Endothelial Cells and Stromal Cells. Tissue Engineering Part A 2013;19(9-10):1209-1222.

14. Vigen M, Ceccarelli J, Putnam AJ. Protease-sensitive PEG hydrogels regulate vascularization in vitro and in vivo. Macromol Biosci 2014;14(10):1368-79.

15. Ghajar CM, Blevins KS, Hughes CC, George SC, Putnam AJ. Mesenchymal stem cells enhance angiogenesis in mechanically viable prevascularized tissues via early matrix metalloproteinase upregulation. Tissue Eng 2006;12(10):2875-88.

16. Rao RR, Peterson AW, Ceccarelli J, Putnam AJ, Stegemann JP. Matrix composition regulates three-dimensional network formation by endothelial cells and mesenchymal stem cells in collagen/fibrin materials. Angiogenesis 2012;15(2):253-64.

17. Fritz H, Wunderer G. Biochemistry and applications of aprotinin, the kallikrein inhibitor from bovine organs. Arzneimittel-Forschung 1983;33(4):479-494.

18. Mühleder S, Pill K, Schaupper M, Labuda K, Priglinger E, Hofbauer P, Charwat V, Marx U, Redl H, Holnthoner W. The role of fibrinolysis inhibition in engineered vascular networks derived from endothelial cells and adipose-derived stem cells. Stem Cell Research & Therapy 2018;9(1):35.

19. Lutolf MP, Lauer-Fields JL, Schmoekel HG, Metters AT, Weber FE, Fields GB, Hubbell JA. Synthetic matrix metalloproteinase-sensitive hydrogels for the conduction of tissue regeneration: Engineering cell-invasion characteristics. Proceedings of the National Academy of Sciences 2003;100(9):5413-5418.

20. McNulty AL, Weinberg JB, Guilak F. Inhibition of matrix metalloproteinases enhances in vitro repair of the meniscus. Clin Orthop Relat Res 2009;467(6):1557-67.

21. Flory PJ. Principles of polymer chemistry. Ithaca,: Cornell University Press; 1953. 672 p. p.

22. Chen X, Aledia AS, Ghajar CM, Griffith CK, Putnam AJ, Hughes CC, George SC. Prevascularization of a fibrin-based tissue construct accelerates the formation of functional anastomosis with host vasculature. Tissue engineering. Part A 2009;15(6):1363-1371.

23. Stevens KR, Scull MA, Ramanan V, Fortin CL, Chaturvedi RR, Knouse KA, Xiao JW, Fung C, Mirabella T, Chen AX and others. In situ expansion of engineered human liver tissue in a mouse model of chronic liver disease. Science Translational Medicine 2017;9(399).

24. Rafii S, Butler JM, Ding B-S. Angiocrine functions of organ-specific endothelial cells. Nature 2016;529(7586):316-325.

25. Bezenah JR, Kong YP, Putnam AJ. Evaluating the potential of endothelial cells derived from human induced pluripotent stem cells to form microvascular networks in 3D cultures. Scientific reports 2018;8(1):2671.

26. Pill K, Melke J, Mühleder S, Pultar M, Rohringer S, Priglinger E, Redl HR, Hofmann S, Holnthoner W. Microvascular Networks From Endothelial Cells and Mesenchymal Stromal Cells From Adipose Tissue and Bone Marrow: A Comparison. Frontiers in Bioengineering and Biotechnology 2018;6:156.

27. Nowak-Sliwinska P, Alitalo K, Allen E, Anisimov A, Aplin AC, Auerbach R, Augustin HG, Bates DO, van Beijnum JR, Bender HR and others. Consensus guidelines for the use and interpretation of angiogenesis assays. Angiogenesis 2018.

28. Yana I, Sagara H, Takaki S, Takatsu K, Nakamura K, Nakao K, Katsuki M, Taniguchi S, Aoki T, Sato H and others. Crosstalk between neovessels and mural cells directs the site-specific expression of MT1-MMP to endothelial tip cells. J Cell Sci 2007;120(Pt 9):1607-14.

29. Turk BE, Huang LL, Piro ET, Cantley LC. Determination of protease cleavage site motifs using mixture-based oriented peptide libraries. Nature Biotechnology 2001;19(7):661-667.

30. Patterson J, Hubbell JA. Enhanced proteolytic degradation of molecularly engineered PEG hydrogels in response to MMP-1 and MMP-2. Biomaterials 2010;31(30):7836-7845.

31. Pratt AB, Weber FE, Schmoekel HG, Müller R, Hubbell JA. Synthetic extracellular matrices for in situ tissue engineering. Biotechnology and Bioengineering 2004;86(1):27-36.

32. van Hinsbergh VW, Collen A, Koolwijk P. Role of fibrin matrix in angiogenesis. Ann N Y Acad Sci 2001;936:426-37.

33. Minami T, Sugiyama A, Wu SQ, Abid R, Kodama T, Aird WC. Thrombin and phenotypic modulation of the endothelium. Arterioscler Thromb Vasc Biol 2004;24(1):41-53.

34. Daviran M, Longwill SM, Casella JF, Schultz KM. Rheological characterization of dynamic remodeling of the pericellular region by human mesenchymal stem cell-secreted

enzymes in well-defined synthetic hydrogel scaffolds. Soft Matter 2018;14(16):3078-3089-3089.

35. Schultz KM, Kyburz KA, Anseth KS. Measuring dynamic cell–material interactions and remodeling during 3D human mesenchymal stem cell migration in hydrogels. Proceedings of the National Academy of Sciences 2015;112(29):E3757-E3764-E3764.

36. Raeber GP, Lutolf MP, Hubbell JA. Molecularly Engineered PEG Hydrogels: A Novel Model System for Proteolytically Mediated Cell Migration. Biophysical Journal 2005;89(2):1374-1388.

37. Cesarman-Maus G, Hajjar KA. Molecular mechanisms of fibrinolysis. Br J Haematol 2005;129(3):307-21.

38. Sokic S, Papavasiliou G. Controlled Proteolytic Cleavage Site Presentation in Biomimetic PEGDA Hydrogels Enhances Neovascularization In Vitro. Tissue Engineering Part A 2012;18(23-24):2477-2486.

39. Blache U, Vallmajo-Martin Q, Horton ER, Guerrero J, Djonov V, Scherberich A, Erler JT, Martin I, Snedeker JG, Milleret V and others. Notch-inducing hydrogels reveal a perivascular switch of mesenchymal stem cell fate. EMBO Rep 2018.

40. Ramos-DeSimone N, Hahn-Dantona E, Sipley J, Nagase H, French DL, Quigley JP. Activation of matrix metalloproteinase-9 (MMP-9) via a converging plasmin/stromelysin-1 cascade enhances tumor cell invasion. J Biol Chem 1999;274(19):13066-76.

41. Tarui T, Majumdar M, Miles LA, Ruf W, Takada Y. Plasmin-induced migration of endothelial cells. A potential target for the anti-angiogenic action of angiostatin. J Biol Chem 2002;277(37):33564-70.

42. Yayama K, Kunimatsu N, Teranishi Y, Takano M, Okamoto H. Tissue kallikrein is synthesized and secreted by human vascular endothelial cells. Biochim Biophys Acta 2003;1593(2-3):231-8.

43. Zollner H. Handbook of enzyme inhibitors. Weinheim, Federal Republic of Germany ; New York, NY, USA: VCH; 1993.

44. Phelps EA, Landázuri N, Thulé PM, Taylor RW, García AJ. Bioartificial matrices for therapeutic vascularization. Proceedings of the National Academy of Sciences 2010;107(8):3323-3328.

45. Phelps EA, Templeman KL, Thulé PM, García AJ. Engineered VEGF-releasing PEG–MAL hydrogel for pancreatic islet vascularization. Drug Delivery and Translational Research 2015;5(2):125-136.

46. Sokic S, Christenson MC, Larson JC, Appel AA, Brey EM, Papavasiliou G. Evaluation of MMP substrate concentration and specificity for neovascularization of hydrogel scaffolds. Biomaterials Science 2014;2(10):1343-1354.

47. Turturro MV, Christenson MC, Larson JC, Young DA, Brey EM, Papavasiliou G. MMP-Sensitive PEG Diacrylate Hydrogels with Spatial Variations in Matrix Properties Stimulate Directional Vascular Sprout Formation. PLoS ONE 2013;8(3).

48. Trappmann B, Baker BM, Polacheck WJ, Choi CK, Burdick JA, Chen CS. Matrix degradability controls multicellularity of 3D cell migration. Nature Communications 2017;8(1):371.

49. Peters EB, Christoforou N, Leong KW, Truskey GA, West JL. Poly(Ethylene Glycol) Hydrogel Scaffolds Containing Cell-Adhesive and Protease-Sensitive Peptides Support Microvessel Formation by Endothelial Progenitor Cells. Cellular and Molecular Bioengineering 2016;9(1):38-54.

FIGURE CAPTIONS

Fig 1: Aprotinin acts synergistically with GM6001 to inhibit vasculogenesis in endothelial cell (EC) co-cultures with dermal fibroblasts (DFs) and lung fibroblasts (LFs) but not in co-cultures with bone-marrow mesenchymal stem cells (MSCs) in 2.5 mg/mL fibrin hydrogels. Representative images of capillary-like networks formed in EC-DF co-cultures after 7 d with indicated inhibitor concentrations are shown stained with the endothelial-selective lectin from *Ulex europaeus* (UEA, red) to highlight networks (A). Scale bar = 500 μm. Multiple images at prespecified locations were acquired for each condition for co-cultures of ECs and DFs (B), LFs (C), or MSCs (D) for 3 independent experiments and network lengths were quantified per volume as outlined in the methods. Two-way ANOVA (GM6001, aprotinin, interaction) results: EC-DF ($p < 0.0001$, $p = 0.0218$, $p = 0.0349$), EC-LF ($p < 0.0001$, $p = 0.0059$, $p = 0.0009$), EC-MSC ($p < 0.0001$, $p = 0.0177$, $p = 0.459$).

Fig 2: Design of MMP- and plasmin-selective PEG-VS hydrogels. We designed PEG-VS hydrogel scaffold systems with selective protease sensitivity by crosslinking multiple-arm PEG-VS with dithiol peptides with selective sensitivity to plasmin or MMPs (A). Hydrogels were crosslinked, swollen in PBS overnight, exposed to plasmin (5 mU/mL), and at indicated times, characterized by shear rheology. Hydrogels crosslinked with YKNR were readily degradable by plasmin as measured by shear rheology, whereas VPMS and Y_D-KN_D-R crosslinked hydrogels were insensitive to plasmin (B).

Fig 3: Capillary morphogenesis is severely restricted in YKNR hydrogels regardless of crosslinking density. UEA (red) images from the centers of the constructs (see methods) are shown for loose (27 mg/mL PEG-VS) and dense (40 mg/mL) VPMS, YKNR, and Y_{D}-KN_{D}-R crosslinked hydrogels. Capillary-like networks formed in EC-DF co-cultures at all concentrations of PEG-VS when crosslinked with VPMS. In YKNR hydrogels, limited vessel formation was only observed in the softest (27 mg/mL) hydrogel formulation. No vessel formation was observed in non-degradable hydrogels (A). Scale bar: 500 μm. Vessel network length was quantified in each scaffold (*: $p < 0.0009$ compared with Y_{D}-KN_{D}-R at fixed concentration, #: $p < 0.008$ compared with 27 mg/mL VPMS) (B). Peptide identity did not influence the shear modulus of hydrogels (two-way ANOVA: $p = 0.40$) (C).

Fig 4: Reduced crosslinking density allows for fibroblast spreading in YKNR crosslinked PEG-VS hydrogels. ECs and DFs were encapsulated in PEG-VS hydrogels with varying peptide identity and crosslinking density, controlled by initial PEG-VS concentration. UEA (red), phalloidin (green), and DAPI (blue) co-stained images from the centers of the constructs are shown for loose (27 mg/mL PEG-VS) and dense (40 mg/mL) VPMS, YKNR, and Y_{D}-KN_{D}-R crosslinked hydrogels (A). Fibroblasts are phalloidin positive but UEA negative. Scale bar: 100 μm. Circularity was quantified (see methods) as a measure of cell spreading in loose (27 mg/mL PEG-VS), intermediate (32 mg/mL), and dense (40 mg/mL) crosslinked hydrogels (*: $p \leq 0.003$ for comparison shown) (B).

Fig 5: Hydrogels with crosslinks sensitive to either plasmin or MMPs did not enhance capillary morphogenesis. PEG-VS hydrogels were crosslinked with a concatenated peptide containing both VPMS and YKNR sequences and used to form scaffolds in which each crosslink was susceptible to either MMPs or plasmin (A). Dense PEG-VS hydrogels were crosslinked with the dual susceptible peptide, swollen in PBS overnight, exposed to indicated proteases, and at indicated times, characterized by shear rheology (B). EC-DF co-cultures were generated in intermediate-crosslinked (32 mg/mL PEG-VS) scaffolds crosslinked with either VPMS or dual-susceptible peptides (C-F). Network structure of these scaffolds, assessed by shear rheology, did not depend on crosslinking peptide ($p = 0.36$) (C). Vessel density, quantified after 7 d, was similar for VPMS and dual susceptible peptides ($p = 0.65$) (D). Cell spreading was estimated by projected cell area per volume and did not differ for VPMS and dual susceptible peptides ($p = 0.11$) (E). There were no differences in cell density after 7 d, measured by automated counting of DAPI stained nuclei per volume ($p = 0.63$) (F).

Fig 6: Cooperative GM6001 and aprotinin inhibition is abolished in VPMS crosslinked hydrogels. EC-DF co-cultures were generated in intermediate-crosslinked (32 mg/mL PEG-VS) hydrogels and cultured for 7 d in the presence of protease inhibitors GM6001 (concentration shown) or aprotinin (2.2 μM). Representative images stained with UEA (red) under indicated conditions are shown (A). Scale bar: 500 μm. Vessel density was quantified for each condition (B). Two-way ANOVA (GM6001, aprotinin, interaction) results: ($p < 0.0003$, $p = 0.21$, $p = 0.75$).

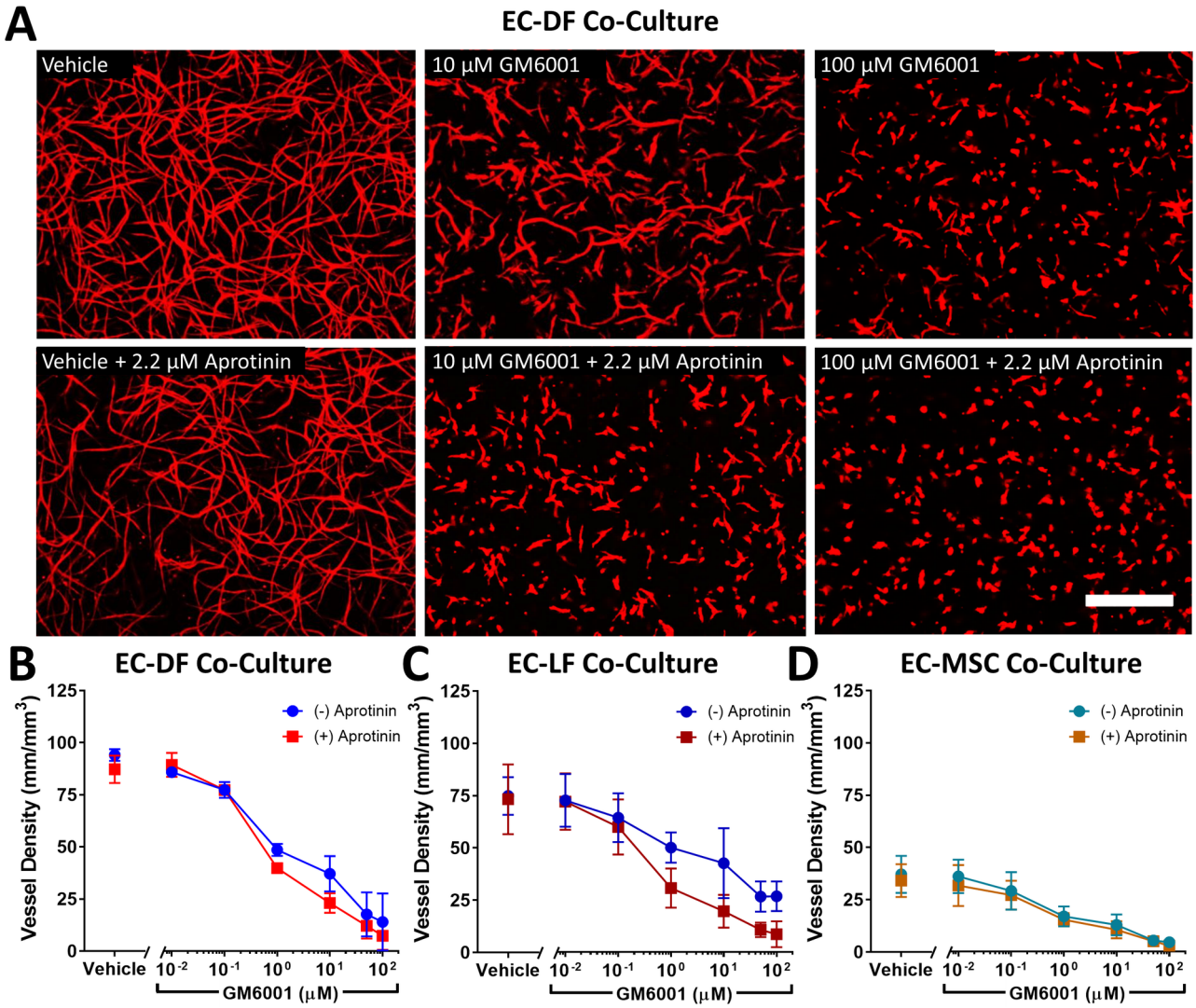

JBMB_34341_Fig 1.TIF

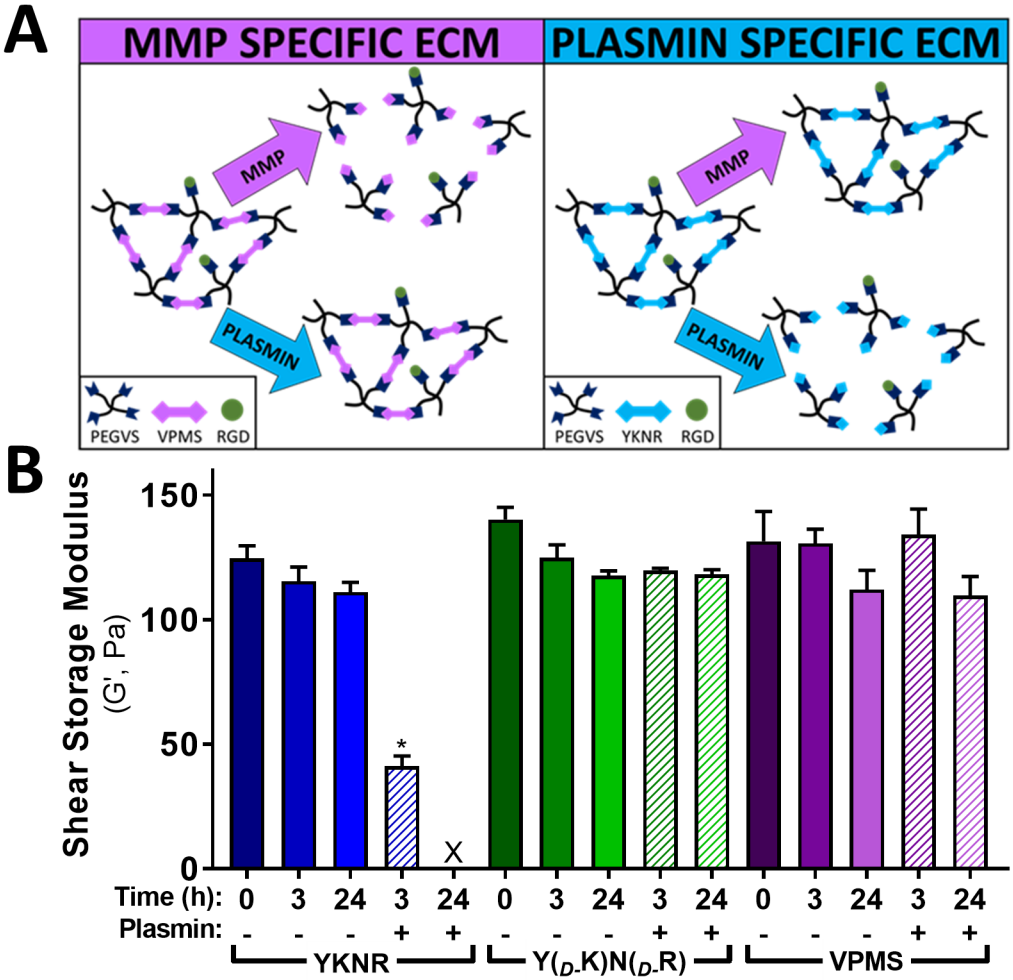

JBMB_34341_Fig 2.TIF

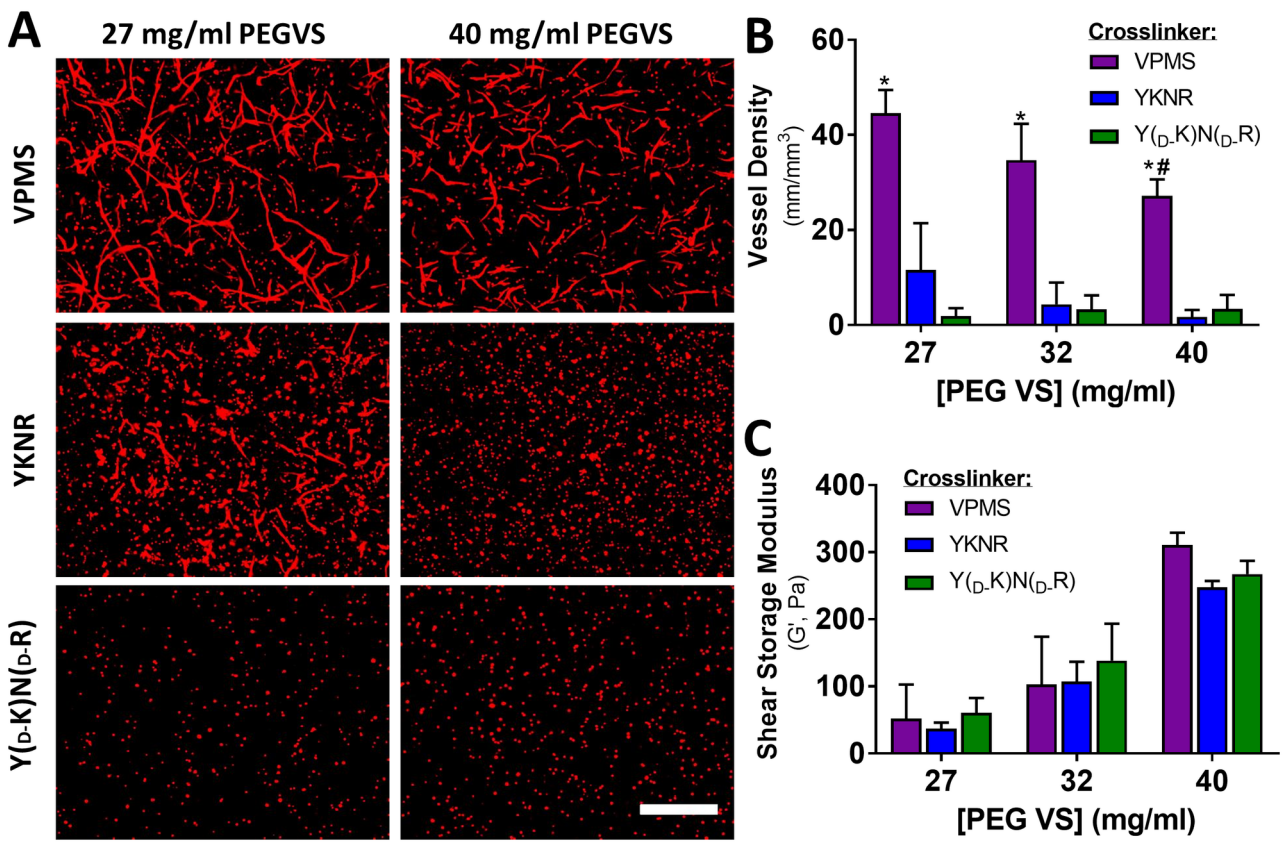

JBMB_34341_Fig 3.TIF

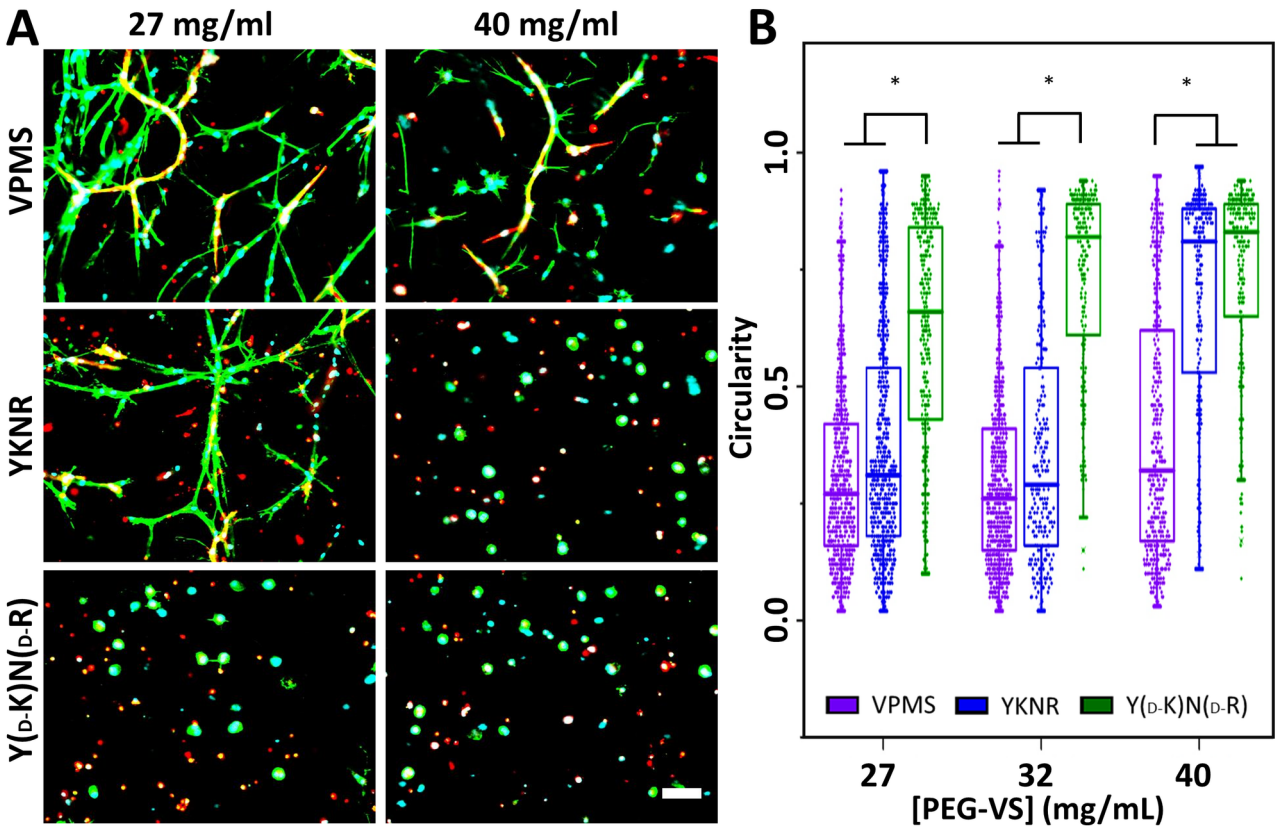

JBMB_34341_Fig 4.TIF

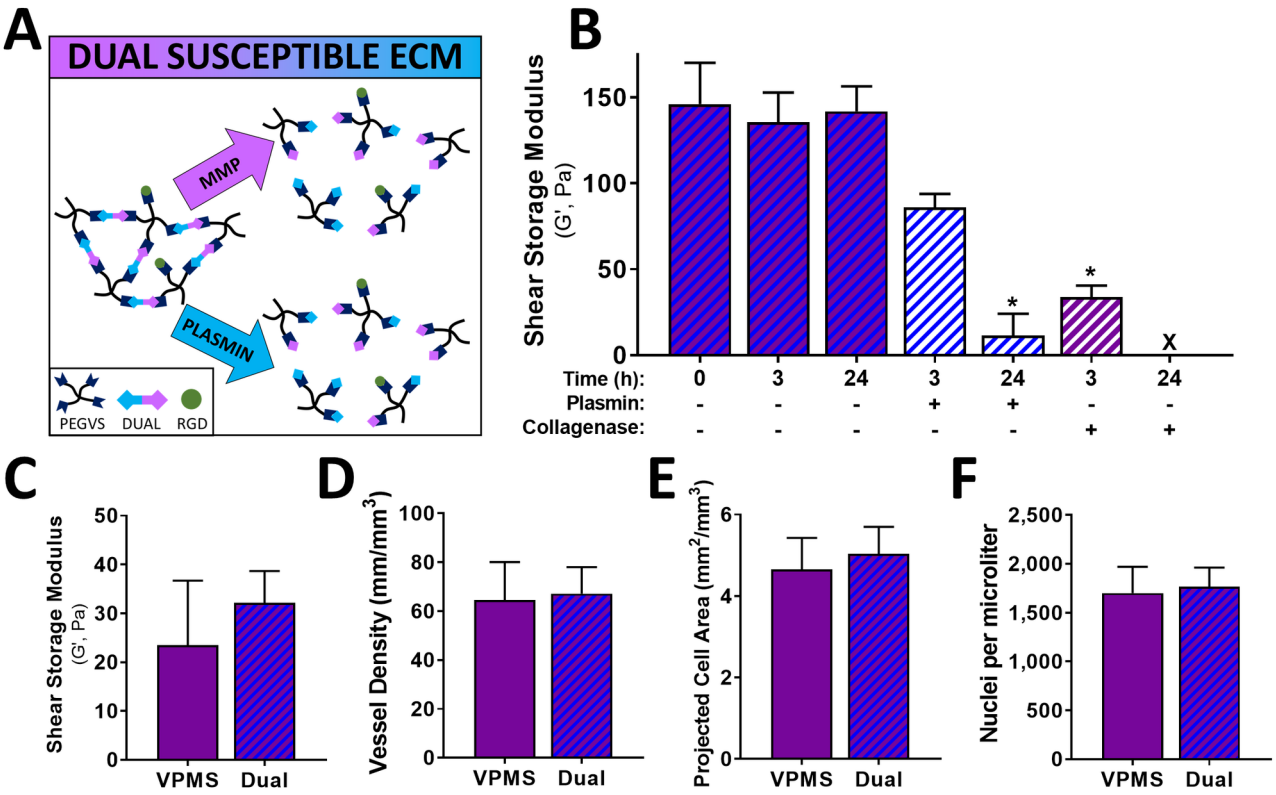

JBMB_34341_Fig 5.TIF

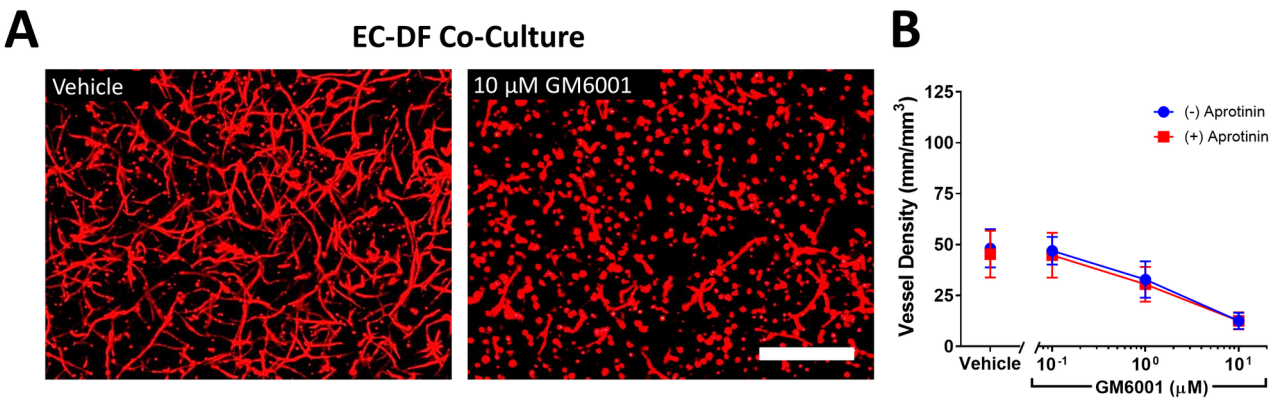

JBMB_34341_Fig 6.TIF